Systematics of nuclear ground-state properties of Sr isotopes by covariant density functional theory

Yuan Tian and Ying Cui
China Institute of Atomic Energy, Beijing 102413, P.R. China

(Received 23 January 2013; revised manuscript received 15 April 2013; published 22 May 2013)

The hyperfine structure and isotope shifts of Sr isotopes, both even-even and odd-even nuclei, are studied in the covariant density functional theory with the new parameter set DD-PC1. Pairing correlation is treated using the Bogoliubov model with a separable form of the pairing interaction. Spin parity, charge radii, two-neutron separation energies, and pairing energies of ground states are calculated and compared with experimental data. We find a shape transition at $N \approx 60$ in charge radii and spin parity, which are consistent with each other and generally agree with experiments. Although the nuclear masses are not very sensitive to these shape changes, odd-even mass differences and pairing effects are very important for study of the shape transition and shape coexistence phenomena in Sr isotopes.

DOI: 10.1103/PhysRevC.87.057305 PACS number(s): 21.60.Jz, 21.10.Dr, 21.30.Fe, 27.60.+j

With new generations of radioactive beam facilities in many countries around the world, experimental and theoretical studies of the properties of nuclear shape evolution as the number of neutron changes is one of the most active and fruitful areas of research in nuclear physics today. In recent decades, several measurements on isotopes with $Z = 36$–40 [1–5] have found a sudden shape transition at $N \approx 60$, but the nature of this transition remains disputed. On the theoretical side, both phenomenological models [6,7] and microscopical models [8–11] have been used to study these isotopes. Most of these models can identify the shape evolution around $N \approx 60$ corresponding to the competition between the prolate and the oblate minimum; the ground states depend on the details of calculations. One of the major goals of the current study is to try to understand the uncertainties in the extrapolation of the pairing strength towards shape coexistence.

Strontium isotopes, with 38 protons, belong to the $Z = 40$ subshell closure, which has a rapid variation of nuclear ground-state properties as a function of the neutron number towards both sides of the line of β stability [5,12]. The charge radius decreases smoothly form the neutron-deficient side, $N \approx Z = 38$, to the neutron shell closure, $N = 50$, then an almost-linear increase is followed by a strong discontinuity at $N = 59$–60. This means that the ground states of Sr isotopes with N ranging around the magic number $N = 50$ are weakly deformed, but they undergo two shape transitions, from nearly spherical to well-deformed deformations, on both the neutron-deficient and the neutron-rich sides.

At present, covariant density functional theory (DFT) based on the mean-field theory provides a very reasonable concept for a universal description of nuclei all over the periodic table [13,14]. Relativistic models incorporate Lorentz invariance, connecting in a consistent way the spin and spatial degrees of freedom of the nucleus, and thus provide a relatively simple phenomenological description for many nuclear properties using only a few phenomenological parameters. In this framework, there are several popular parameter sets, including NL3 [15] and PK1 [16] for the nonlinear RMF model, DD-ME2 [17] and PKDD [16] for the density-dependent RMF model, and density-dependent point-coupling interaction (DD-PC1) [18] and PC-PK1 [19] for the point-coupling RMF model. Among these parameter sets, the DD-PC1 was proposed very recently by additional fitting to the masses of 64 axially deformed nuclei. Compared with the available data, DD-PC1 provides a very good agreement with the properties of spherical and deformed medium-heavy and heavy nuclei, including binding energies (BEs), charge radii, deformation parameters, neutron skin thickness, and excitation energies of giant multipole resonances.

In most DFT calculations, the pairings have often been taken into account in a very phenomenological way in the BCS model with the monopole pairing force, adjusted to the experimental odd-even mass differences. In many cases, however, this approach presents only a poor approximation. The physics of weakly bound nuclei, in particular, necessitates a unified and self-consistent treatment of mean-field and pairing correlations. This has led to the formulation and development of the relativistic Hartree-Bogoliubov (RHB) model, which represents a relativistic extension of the conventional Hartree-Fock-Bogoliubov framework. In most applications of the RHB model simple phenomenological pairing forces such as the monopole force taking into account pairing correlations only in the $J = 0$ channel or density-dependent δ interaction (DDDI) [20–22] where additional simplifying assumptions have to be introduced as, for instance, a pairing window. Gogny forces [23–25] with finite range are considered to provide the best phenomenological description of pairing correlations in nuclei. However, because of their numerical complexity, they are applied only by a rather limited number of groups in the literature.

Recently, we have introduced a separable form of the pairing force for RHB calculations in finite nuclei [26–30]. The force is separable in momentum space and is determined by two parameters that are adjusted to reproduce the pairing gap of the Gogny force in symmetric nuclear matter. Using Talmi-Moshinsky techniques [31–33], it can be represented as a series of separable terms in a harmonic oscillator basis. Although different from the Gogny force, the corresponding effective pairing interaction has been shown to reproduce with a high accuracy pairing gaps and energies calculated with the original Gogny force, in both spherical and deformed nuclei. In particular, this approach retains the basic advantage of the finite-range Gogny force, and the numerical calculation is much simpler. Therefore, in this work, we study the ground-state properties of Sr isotopes in the framework of the self-consistent RHB approximation based on the DD-PC1 parameter set together with the separable pairing force.

In the framework of covariant DFT, the energy functional of the RHB model depends not only on the density matrix $\hat{\rho}$ and the meson fields ϕ_m, but also on the pairing tensor

$$E_{\mathrm{RHB}}[\hat{\rho}, \phi_m, \hat{\kappa}] = E_{\mathrm{RMF}}[\hat{\rho}, \phi_m] + E_{\mathrm{pair}}[\hat{\kappa}], \tag{1}$$

where $E_{\mathrm{RMF}}[\hat{\rho}, \phi_m]$ is the RMF functional based on the DD-PC1 [18], and the pairing energy $E_{\mathrm{pair}}[\hat{\kappa}]$ is given by

$$E_{\mathrm{pair}}[\hat{\kappa}] = \tfrac{1}{4}\mathrm{Tr}[\hat{\kappa}^* V^{pp} \hat{\kappa}]. \tag{2}$$

V^{pp} denotes the two-body pairing interaction. Here we use the separable form of the pairing force:

$$\langle k | V_{\mathrm{sep}}^{^1S_0} | k' \rangle = -G p(k) p(k'). \tag{3}$$

A simple Gaussian ansatz $p(k) = e^{-a^2k^2}$ is assumed. In Ref. [28] the two parameters G and a have been fitted to the density dependence of the gap $\Delta(k_F)$ of the Gogny D1S [34] in nuclear matter. The obtained values for the parameters are $G = 728$ MeV fm^3 and $a = 0.644$ fm.

Odd-A nuclei can be considered as an even-even core plus an unpaired nucleon (or quasiparticle). Using the equal filling approximation (EFA) [35,36], the unpaired nucleon is treated on an equal footing with its time-reversed state by setting half a nucleon in a given orbital and the other half in the time-reversed partner. For axially deformed nuclei, the spin is simply the projection of the angular momentum along the symmetry axis for the last occupied proton or neutron level, when this level is occupied by a single nucleon. For spherical nuclei with degenerate levels, the nuclear spin is defined as the maximum value of j_z, which is $|j|$.

The mean-square charge radius is calculated as [37,38]

$$r_c^2 = \frac{1}{Z}\int r^2 d^3 n_p(r) + r_p^2 + \frac{N}{Z} r_n^2 - r_{\mathrm{c.m.}}^2, \tag{4}$$

where $n_p(r)$ is the point-proton density and $r_p^2 = 0.63$ fm^2 and $r_n^2 = -0.12$ fm^2 are the rms proton and neutron charge radii, respectively. The center-of-mass correction is computed as $r_{\mathrm{c.m.}}^2 = 3\hbar/2m\omega A$ fm^2, with $\omega = 1.85 + 35.5/A^{1/3}$ MeV. We show in Fig. 1 a comparison of calculated and experimental charge radii, plotted as $\delta\langle r_c^2\rangle^{50,N} = \langle r_c^2\rangle^N - \langle r_c^2\rangle^{50}$.

The potential energy surface in the plane of deformation variables is obtained by imposing a quadratic constraint on the mass quadrupole moments,

$$\langle H\rangle + C_{20}(Q_{20} - q_{20})^2, \tag{5}$$

where $\langle H\rangle$ is the total energy, q_{20} is a constrained value of the quadrupole moments, and C_{20} is the corresponding stiffness constant [39]. The quadrupole Q_{20} moments for neutrons and protons are calculated using the expressions

$$Q_{20} = \langle 2r^2 P_2(\cos\theta)\rangle_{n,p} = \langle 2z^2 - x^2 - y^2\rangle. \tag{6}$$

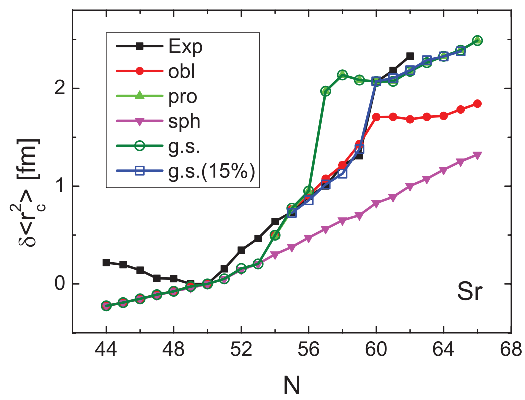

FIG. 1. (Color online) Calculated $\delta\langle r_c^2\rangle$ in Sr isotopes compared to experimental data from Ref. [41]. Results for oblate, prolate, and spherical minima are displayed by different symbols (see the legend). Open circles and squares correspond to ground-state results with different pairing strengths.

The conventional deformation parameter β is obtained from the calculated quadrupole moments through

$$Q_{20} = \sqrt{\frac{16\pi}{5}}\frac{3}{4\pi} A R_0^2 \beta, \tag{7}$$

with $R_0 = 1.2A^{1/3}$ (fm).

In this article, we also calculate the three-point neutron pairing energy (Δ_n^3) and two-neutron separation energy (S_{2n}) of the Sr isotope, which can be easily obtained from the BEs:

$$\Delta_n^3(N,Z) = \tfrac{1}{2}(\mathrm{BE}(N-1,Z) - 2\mathrm{BE}(N,Z) + \mathrm{BE}(N+1,Z), \tag{8}$$

$$S_{2n}(N,Z) = \mathrm{BE}(N-2,Z) - \mathrm{BE}(N,Z). \tag{9}$$

The ground-state properties of Sr isotopes from $N = 44$ to $N = 66$ with both even-even and even-odd nuclei have been calculated with RHB theory with DD-PC1 [18] and the separable pairing force [27].

The experimental spin-parity assignments in odd-A Sr-isotopes [40] are listed in the third column in Table I. They are compared to the one-quasiparticle states calculated by

TABLE I. Experimental spin-parity assignments [40] compared with RHB-EFA results for one-quasiparticle states in odd-A Sr isotopes.

A	N	Expt. [40]	Spherical	Oblate	Prolate
83	45	$7/2+$ $(9/2+)$	$g_{9/2}$		
85	47	$9/2+$	$g_{9/2}$		
87	49	$9/2+$	$g_{9/2}$		
89	51	$5/2+$	$d_{5/2}$		
91	53	$5/2+$	$d_{5/2}$		
93	55	$5/2+$	$d_{5/2}$	$3+[402]$	$3+[422]$
95	57	$1/2+$		$1+[400]$	$3-[541]$
97	59	$1/2+$		$1+[400]$	$9+[404]$
99	61	$3/2+$			$3+[411]$
101	63	$5/2-$			$5-[532]$
103	65				$5+[413]$

the RHB-EFA. In our calculations, Sr isotopes evolve from spherical shapes in $^{83-91}$Sr around $N = 50$ with the spherical $g_{9/2}$ and $d_{5/2}$ shells involved, to slightly deformed shapes in ^{93}Sr, and, finally, to shape coexistence in $^{95-103}$Sr. In the lighter isotopes the two spherical shells give the same ground states as the experimental. For slightly deformed nuclei, the experimental ground states are $5/2+$ in ^{93}Sr. In ^{93}Sr, the potential energy surface is very flat. Although the oblate minimum ($\beta \approx -0.2$) with $3+[402]$ is slightly deeper, the spherical minimum with $d_{5/2}$ is very close and it is consistent with the measurement. For $N \geqslant 57$ Sr isotopes, there are two minima, for the oblate and prolate shapes. The competition between these two minima is very sensitive to the calculations. In our work, the oblate ground state in ^{95,97}Sr is $1+[400]$, and the prolate ground state is $3-[541]$ and $9+[404]$, respectively. Compared with the measurements, these two nuclei should be oblate deformed. But our results prefer the prolate ground state, as $N = 58$ is a subshell structure on the prolate side for our calculation. For the higher isotopes, the prolate ground states with $3+[411]$ in ^{99}Sr and $5-[532]$ in ^{101,103}Sr are in agreement with the experiment.

Figure 1 displays the evolution of the nuclear charge radii in Sr isotopes, where the experimental [41] and the calculated charge radii corresponding to the oblate, prolate, and spherical including both even-even and odd-A isotopes are plotted as functions of the neutron number. The charge radii decrease until the shell closure at $N = 50$. After that, an almost-linear increase is followed by a strong discontinuity at $N = 59$–60.

For $44 \leqslant N \leqslant 55$, our calculations predict that these nuclei are soft against deformation. The softness, or the width of the potential energy surface around $\beta = 0$, increases as one departs from the shell closure at $N = 50$. Thus, the actual charge radius of our calculation will increase slightly and be very close to the experimental data if we take account of the contributions of deformed configurations for the ground state.

For neutron-rich ($N \geqslant 56$) nuclei, the axial symmetric calculation provides two minima in both the prolate and the oblate regions. The BE difference between the lowest oblate and the lowest prolate minima is less than 1 MeV for these nuclei. We indicate a sudden increase in the charge radius from $N = 56$ to $N = 57$, which corresponds to the transition from the oblate shape $\beta = -0.2$ (^{94}Sr) to the prolate shape $\beta = 0.5$ (^{95}Sr). As we see in Fig. 1 a jump in the experimental data is observed between $N = 59$ and $N = 60$. However, we do not think this discrepancy is significant, as it is related to the subtle competition between prolate and oblate shapes.

In Fig. 2 we can see the results of two neutron separation energies S_{2n} and three-point neutron pairing energies Δ^3 shown as a function of the neutron number for both even and odd. In general, we reproduce the experimental data reasonably well, which is taken from the mass table [42]. Between $N = 52$ and $N = 54$, the S_{2n} energies are underestimated by the calculations, which are also found in Ref. [10]. In our calculations a change in the tendency is observed from $N = 56$ to $N = 57$, and the three-point neutron pairing energies from $N = 56$ to $N = 59$ are slightly lower than the experimental data.

In general, our calculations for Sr isotopes follow the measurements very well except for the nuclei around $N = 58$.

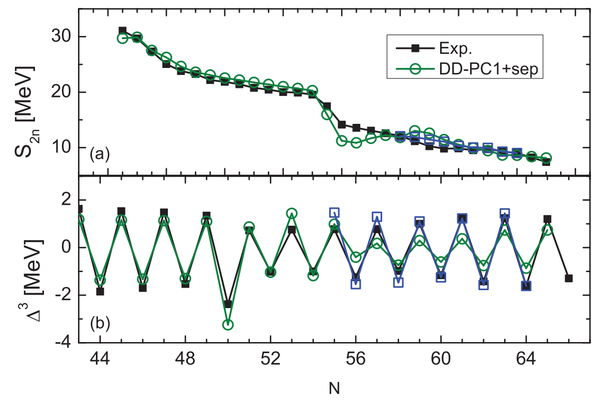

FIG. 2. (Color online) Calculated S_{2n} (a) and Δ^3 (b) compared to experimental data from Ref. [42]. Open squares are the results of S_{2n} and Δ^3 with a higher pairing strength.

Because the effective mass of DD-PC1 is a little small, a subshell structure has been found in the prolate ground state of nuclei around $N = 58$ for our calculations. This special structure makes $N = 58$ a "magic" number on the prolate side, and it becomes more stable than other minima. However, the experimental spin-parity and charge radii have shown us that the oblate minima of these nuclei are the real ground state. The basic idea to solve this problem is to use another parameter set with a large effective mass, such as the Skyrme(SkM*) or Gogny D1S interaction, which we will discuss in the future.

Figure 2(b) shows that the calculated Δ^3 is smaller than the experimental data after $N = 55$. So here we slightly increase the pairing strength (15%) to fit the experimental results [open-square line in Fig. 2(b)] and study the pairing effect on shape coexistence. As Figs. 1 and 2 show, the calculated $\delta\langle r_c^2\rangle$ and two neutron separation energies with larger pairings are much closer to the experimental results, especially for nuclei around $N = 58$. In Fig. 3 we display the potential energy surfaces of ^{96}Sr obtained from a self-consistent RHB calculation based on the parameter set DD-PC1 using a separable pairing with 100% (black) and 115% (red) strengths in the pairing channel. And we find that the ground state of

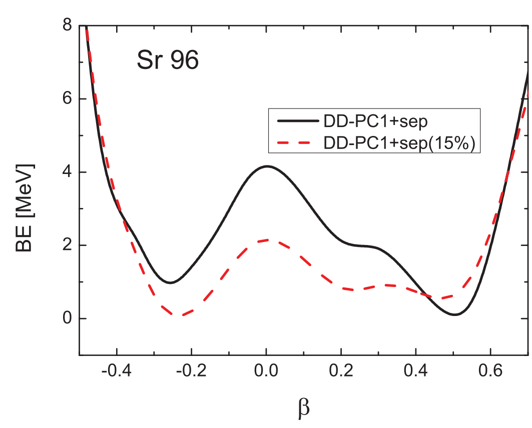

FIG. 3. (Color online) Potential energy surfaces in ^{96}Sr obtained in different pairing schemes (see legend) with DD-PC1 parametrization of the RMF Lagrangian.

TABLE II. Binding energies and charge radii of nuclei around the $N = 58$ subshell with different pairing interactions.

N	β	BE	$\delta\langle r_c^2\rangle$	BE (15%)	$\delta\langle r_c^2\rangle$ (15%)	$\delta\langle r_c^2\rangle$ (exp)
57	Oblate	−810.320	1.075	−811.911	1.018	1.003
	Prolate	−811.294	1.971	−811.192	1.693	
58	Oblate	−816.909	1.214	−818.917	1.128	1.213
	Prolate	−817.764	2.137	−818.385	1.965	
59	Oblate	−821.918	1.431	−822.975	1.378	1.312
	Prolate	−822.750	2.086	−822.906	2.071	

^{96}Sr jumps from prolate to oblate. In Table II, we compare the ground-state properties of nuclei around $N = 58$ with different pairing strengths. Compared with the experimental $\delta\langle r_c^2\rangle$ and spin-parity results in Sec. III A, the oblate minimum should be the ground state for these three nuclei. The separable pairing interaction is introduced by reproducing the pairing properties of the Gogny D1S in nuclear matter. And we have proved that the separable pairing interaction can give the same pairing properties as the Gogny D1S in both spherical and deformed nuclei [26–30]. Compared with the experimental Δ^3, the Gogny D1S is obviously too small for these nuclei. And the same problem occurs in the HFB calculation with the Gogny D1S; it cannot reproduce the experimental results for these three nuclei either [43]. In this paper, by increasing the pairing strength slightly, we reproduce not only the experimental Δ^3, but also other ground states of nuclei around $N = 58$, such as the charge radii, two-neutron separation energies, and spin-parity properties of odd-A nuclei.

In summary we have studied the ground-state properties of Sr isotopes on the neutron-rich side. We have analyzed various sensitive nuclear observables, such as the charge radius, two-neutron separation energy, neutron pairing energy, and spin parity of the ground states in a search for signatures of shape transitions. We have found that the charge radii and the spin parity are very sensitive to shape changes. In addition, although the pairing cannot change the level density, the effect is very important and should be treated very carefully.

Y. Tian would like to thank Prof. Peter Ring and Prof. Zhong-Yu Ma for helpful discussions. This research was supported by the National Natural Science Foundation of China under Grant No. 11075213.

[1] C. Thibault, F. Touchard, S. Büttgenbach, R. Klapisch, M. de Saint Simon, H. T. Duong, P. Jacquinot, P. Juncar, S. Liberman, P. Pillet *et al.*, Phys. Rev. C **23**, 2720 (1981).

[2] P. Campbell, H. L. Thayer, J. Billowes, P. Dendooven, K. T. Flanagan, D. H. Forest, J. A. R. Griffith, J. Huikari, A. Jokinen, R. Moore *et al.*, Phys. Rev. Lett. **89**, 082501 (2002).

[3] R. Meyer, E. Monnand, J. Pinston, F. Schussler, I. Ragnarsson, B. Pfeiffer, H. Lawin, G. Lhersonneau, T. Seo, and K. Sistemich, Nucl. Phys. **439**, 510 (1985).

[4] H. Mach, F. Wohn, G. Molnr, K. Sistemich, J. C. Hill, M. Moszyski, R. Gill, W. Krips, and D. Brenner, Nucl. Phys. **523**, 197 (1991).

[5] F. Buchinger, E. B. Ramsay, E. Arnold, W. Neu, R. Neugart, K. Wendt, R. E. Silverans, P. Lievens, L. Vermeeren, D. Berdichevsky *et al.*, Phys. Rev. C **41**, 2883 (1990).

[6] A. Kumar and M. R. Gunye, Phys. Rev. C **32**, 2116 (1985).

[7] F. R. Xu, P. M. Walker, and R. Wyss, Phys. Rev. C **65**, 021303 (2002).

[8] M. Bender, G. F. Bertsch, and P.-H. Heenen, Phys. Rev. C **73**, 034322 (2006).

[9] M. Bender, G. F. Bertsch, and P.-H. Heenen, Phys. Rev. C **78**, 054312 (2008).

[10] R. Rodrguez-Guzmn, P. Sarriguren, L. M. Robledob, and S. Perez-Martin, Phys. Lett. B **691**, 202 (2010).

[11] J. Xiang, Z. Li, Z. Li, J. Yao, and J. Meng, Nucl. Phys. **873**, 1 (2012).

[12] P. Lievens, L. Vermeeren, R. E. Silverans, E. Arnold, R. Neugart, K. Wendt, and F. Buchinger, Phys. Rev. C **46**, 797 (1992).

[13] M. Bender, P.-H. Heenen, and P.-G. Reinhard, Rev. Mod. Phys. **75**, 121 (2003).

[14] D. Vretenar, A. Afanasjev, G. Lalazissis, and P. Ring, Phys. Rep. **409**, 101 (2005).

[15] G. A. Lalazissis, J. König, and P. Ring, Phys. Rev. C **55**, 540 (1997).

[16] W. Long, J. Meng, N. Van Giai, and S.-G. Zhou, Phys. Rev. C **69**, 034319 (2004).

[17] G. A. Lalazissis, T. Nikšić, D. Vretenar, and P. Ring, Phys. Rev. C **71**, 024312 (2005).

[18] T. Nikšić, D. Vretenar, and P. Ring, Phys. Rev. C **78**, 034318 (2008).

[19] P. W. Zhao, Z. P. Li, J. M. Yao, and J. Meng, Phys. Rev. C **82**, 054319 (2010).

[20] G. Bertsch and H. Esbensen, Ann. Phys. **209**, 327 (1991).

[21] J. Meng and P. Ring, Phys. Rev. Lett. **77**, 3963 (1996).

[22] T. Bürvenich, D. G. Madland, J. A. Maruhn, and P.-G. Reinhard, Phys. Rev. C **65**, 044308 (2002).

[23] J. Dechargé and D. Gogny, Phys. Rev. C **21**, 1568 (1980).

[24] J. Egido and L. Robledo, Nucl. Phys. A **494**, 85 (1989).

[25] T. Gonzalez-Llarena, J. Egido, G. Lalazissis, and P. Ring, Phys. Lett. B **379**, 13 (1996).

[26] Y. Tian and Z. Y. Ma, Chin. Phys. Lett. **23**, 3226 (2006).

[27] Y. Tian, Z. Y. Ma, and P. Ring, Phys. Lett. B **676**, 44 (2009).

[28] Y. Tian, Z. Y. Ma, and P. Ring, Phys. Rev. C **79**, 064301 (2009).

[29] Y. Tian, Z. Y. Ma, and P. Ring, Phys. Rev. C **80**, 024313 (2009).

[30] T. Nikšić, P. Ring, D. Vretenar, Y. Tian, and Z.-Yu. Ma, Phys. Rev. C **81**, 054318 (2010).
[31] I. Talmi, Helv. Phys. Acta **25**, 185 (1952).
[32] M. Moshinsky, Nucl. Phys. **13**, 104 (1959).
[33] T. Brody, G. Jacob, and M. Moshinsky, Nucl. Phys. **17**, 16 (1960).
[34] J. Berger, M. Girod, and D. Gogny, Comput. Phys. Commun. **63**, 365 (1991).
[35] S. Perez-Martin and L. M. Robledo, Phys. Rev. C **78**, 014304 (2008).
[36] N. Schunck, J. Dobaczewski, J. McDonnell, J. Moré, W. Nazarewicz, J. Sarich, and M. V. Stoitsov, Phys. Rev. C **81**, 024316 (2010).
[37] J. W. Negele, Phys. Rev. C **1**, 1260 (1970).
[38] J. P. Delaroche, M. Girod, J. Libert, H. Goutte, S. Hilaire, S. Péru, N. Pillet, and G. F. Bertsch, Phys. Rev. C **81**, 014303 (2010).
[39] P. Ring and P. Schuck, *The Nuclear Many-Body Problem*, *Texts and Monographs in Physics* (Springer, Berlin, 1980).
[40] Evaluated Nuclear Structure Data Files (ENSDF); www.nndc.bnl.gov/ensdf.
[41] I. Angeli, At. Data Nucl. Data Tables **87**, 185 (2004).
[42] G. Audi, A. Wapstra, and C. Thibault, Nucl. Phys. A **729**, 337 (2003); The 2003 NUBASE and Atomic Mass Evaluations.
[43] R. Rodriguez-Guzman, P. Sarriguren, and L. M. Robledo, Phys. Rev. C **82**, 044318 (2010).